Jurnal Teknologi

Full Paper

ALL-OPTICAL HYSTERESIS SWITCHING USING MOBIUS CONFIGURATION MICRORING RESONATOR CIRCUIT

Ahmad Fakhrurrazi Ahmad Noorden[a], Azam Mohamad[a], Mahdi Bahadoran[a], Kashif Chaudhary[a], M. S. Aziz[a], Muhammad Arif Jalil[a], Jalil Ali[a*], Preecha Yupapin[b]

[a]Laser Centre, Ibnu Sina ISIR, Universiti Teknologi Malaysia, 81310 UTM Johor Bahru, Johor, Malaysia
[b]Advanced Studies Center, Faculty of Science King Mongkut's Institute of Technology Ladkrabang, Bangkok 10520, Thailand

Article history
Received
10 October 2014
Received in revised form
10 December 2014
Accepted
13 January 2015

*Corresponding author
jalilali@utm.my

Graphical abstract

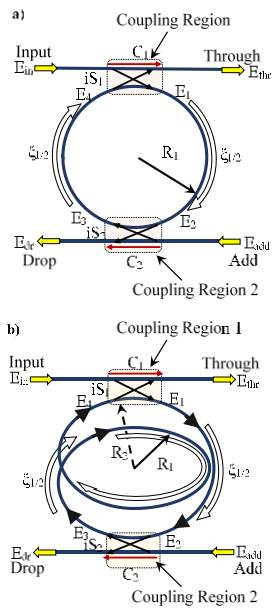

Abstract

The novel twisted ring resonator called add-drop Mobius microring resonator is introduced and modelled with the analytical solution of transfer matrix methods for the generation of optical bistability. Simulated results show that, the add-drop Mobius configuration provides greater phase shift due to the longer length of propagation per roundtrip than add-drop filter configuration. In add-drop Mobius system, drop port generated the optical bistable hysteresis loop with 19.25 mW output switching power and through port generated lower switching power as 5.55 mW. The drop port of the system is found as the suitable port for the operating the all-optical hysteresis switching.

Keywords: Add-drop mobius (ADM) ring resonator, transfer matrix analysis, optical bistability, hysteresis loop

Abstrak

Penyalun cincin novel dipintal dipanggil Mobius penambah-jatuh penyalun cincin mikro diperkenalkan dan dimodelkan dengan penyelesaian analitikal kaedah matriks pindahan untuk penghasilan dwikestabilan optik. Hasil simulasi menunjukkan bahawa, konfigurasi Mobius penambah-jatuh menyediakan anjakan fasa yang lebih besar kerana rambatan panjang yang lebih per-alik daripada konfigurasi penapis penambah-jatuh. Dalam sistem Mobius penambah-jatuh, port jatuh menjana gelung dwikestabil optik dengan 19.25 mW kuasa peralihan output dan port lepasan menjana kuasa peralihan yang lebih rendah dengan 5.55 mW. Port jatuh pada sistem ini didapati sebagai port yang sesuai untuk operasi pensuisan histerisis penyeluruh-optik.

Kata kunci: Penyalun cincin mobius Penambah-jatuh (ADM), analisis matriks pemindahan, dwikestabilan optic, gelung histeresis

1.0 INTRODUCTION

In all-optical signal processing, the optical bistability has received much attention as one of the important optical properties for switching purposes which can be applied as optical transistor application [1]. The optical bistability is a signal property consist of two stable resonance states of transmission signal which possible to obtain from one input signal [2]. Recently, the switching effect of the optical bistability are attracting widespread interest in fields such as

microresonator circuit, communication [3, 4] and optical storage [5]. Several experiments and theoretical simulations have been conducted for enhanced optical bistability which based-on the Fabry-Perot cavities [6], ring cavities [7], and feedback nonlinear fiber loops cavities [8]. However, optical bistability enhancement based on optical microring resonator still required the theoretical and analytical formulation for microscale applications. Felber *et al*. developed the analysis of the optical bistability using graphical-based method which can be used to explain optical bistability behavior in Fabry-Perot system with nonlinear medium by considering the nonlinear Kerr effect [9]. The topological effects of the microring resonator configuration is one of the method to enhance the nonlinarity Kerr effects [10] and increase the optical bistability generation. Yupapin *et al*. establish a PANDA configuration in which can be used to produce all-optical switching from bistability effect [11, 12]. The Mobius configuration has been used as the bandpass filter [13] as wire resonator which possible to be applied in form of optical waveguide resonator [14]. Nowadays, Silicon-On-Insulator (SOI) waveguide has become one of potential medium of integrated circuits technology which emerges in application of optical resonators.

The aim of this work is to enhance the optical bistability by manipulating the topological configuration of microring resonator (MRR) system. The configurations are divided in two types which are optical add-drop filter (ADF) resonator and add-drop Mobius (ADM) resonator. The SOI waveguide properties are used in the iterative formulation and scattering matrix method of both configuration for the bright and dark soliton pulse in launched to the input port and add port of MRR system respectively. The ADM configuration is capable on increase the optical bistability and the optical hysteresis loop of the MRR output signal.

2.0 MICRORING RESONATOR CONFIGURATION

The microring resonator comprises several types of configuration such as all-pass filter [15], add-drop filter (ADF) [16] and PANDA ring resonator [17]. The present work focused on the ADF configuration with lateral coupling of two bus waveguide with one closed loop (ring) waveguide. The SOI material is used with core of Si which embedded inside the SiO_2 cladding as shown in Figure 1 a) and b).

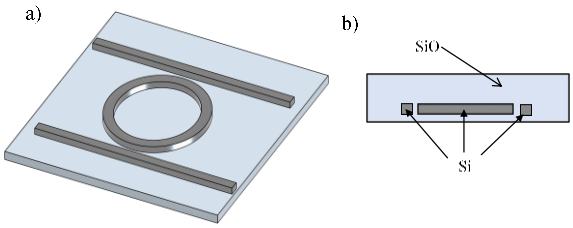

Figure 1 (a) Upper view of SOI microring resonator and (b) Side view of SOI microring resonator

The Mobius type ring waveguide is implemented to obtain a smaller configuration with higher circulation trails in which enhance the nonlinearity of MRR system. The comparison between ADM and ADF design is illustrated as Figure 2.

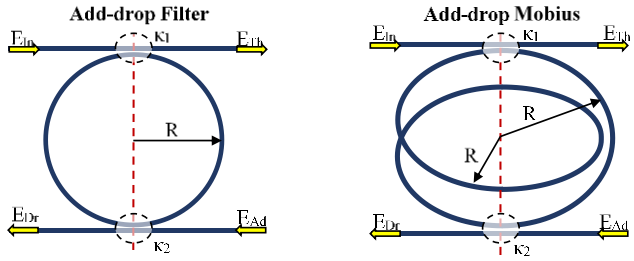

Figure 2 The schematics diagram of ADF and ADM microring resonator system

The iterative programming script have been develop by the derivation of the propagation equation of the electric fields based on the coupled-mode theory with the nonlinear medium consideration of the waveguide properties. The optical bistability is analysed based on the comparison between the simulated output-to-input power relation of electric fields (E_{Th}) for ADM and ADF MRR configurations as shown in Figure 2. The optical bright and dark soliton pulses are applied as input sources for input and add ports to operate the MRR system. The theoretical derivation will be discussed thoroughly in Section 3.

3.0 THEORY AND ANALYTICAL FORMULATION

Grounded with transfer matrix analysis method, the analytical formulation is conducted to produce the propagated electric fields for both configurations of MRR system. The electric field equations are computed for several specific points within the MRR configurations which used to derive the optical transfer functions [18]. Figure 3 a) and b) illustrate the schematics diagrams of the electrics field propagation with the notation of transfer matrix analysis of MRR system for ADF and ADM configurations respectively. The bright and dark [19, 20] soliton pulses used as the input and add ports laser sources (E_{In} nand E_{Add}) respectively with 1.55 μm

centre wavelength which are described in theoretical formulation in Equations (1) and (2).

$$E_{In} = \Upsilon \operatorname{sech}\left(\frac{\Gamma}{\Gamma_0}\right) exp\left[\left(\frac{z}{2L_D}\right) - i\phi(t)\right] \quad (1)$$

$$E_{Add} = \Upsilon \tanh\left(\frac{\Gamma}{\Gamma_0}\right) exp\left[\left(\frac{z}{2L_D}\right) - i\phi(t)\right] \quad (2)$$

The bright and dark soliton equations decribed electric fields of the pulses as E_{In} and E_{Add} which comprised of peak amplitude of the optical field Υ, the propagation distance z and pulse propagation time Γ. The propagation time Γ is obtained based on a moving frame $t - \beta_1 z$ with t is soliton phase shift time. The initial propagation time Γ_0 of the pulses is related to soliton pulses dispersion length as $L_D = T_0 / |\beta_2|$. The dispersion effect have been obtained in parameters β_1 and β_2 which illustrates the first and second orders of Taylor expansion towards the propagation constant and $\phi(t)$ is the optical phase shift [19-21]. The nonlinear Kerr effect have been considered in temporal function of phase shift as

$$\phi(t) = \phi_L + \phi_{NL} = \phi_L + \frac{2\pi n_2 L}{A_{eff}\lambda}|E_0|^2 \quad (3)$$

The temporal function of optical phase shift is defined as the summation of nonlinear ϕ_{NL} and linear ϕ_L phase shift in which the nonlinear part comprised of the nonlinear index which originated from the medium properties of SOI material. The nonlinear Kerr effect is used for describing the nonlinear phase with optical intensity $I = |E_0|^2 / A$ dependent of the nonlinear index. Thus, the refractive index of the medium can be defined as [22].

$$n = n_1 + n_2 I = n_1 + n_2 2n_1\varepsilon_0 c|E_0|^2 \quad (4)$$

The refractive index of the material n can be defined as linear n_1 and nonlinear index n_2 that related with electrical permittivity ε_0 and light speed c. The input soliton pulses from add and input ports are propagated through the bus waveguide and coupled into the ring waveguide as it reach the coupling region as labelled in Figures 3 a) and b).

The coupling phenomenon has been described by the consideration cross and self-coupling parameters within the coupled mode theory equations. The cross iS_1 and self-coupling C_1 [23] can be defined as the portion of the light that coupled across waveguide and remain in initial waveguide respectively which can be stated as

$$iS_1 = \sqrt{(1-\gamma_1)(\kappa_1)} \quad (5)$$

$$C_1 = \sqrt{(1-\gamma_1)(1-\kappa_1)} \quad (6)$$

The summation of coupling parameters indicates the total amount of light which travel before reach the coupling region. The full portion of light can be defined as $|iS_1|^2 + |C_1|^2 = 1$ when the coupler is considered as lossless, where κ_1 is coupling coefficient and γ_1 is coupler loss. The coupled of the evanescence wave of the incident light pulses will exhibit the coupler loss while travelling across the waveguide. The travelling pulse will exhibit two coupling phenomenon of evanescence wave as the pulse propagates within the ring waveguide from electric field E_1 to the second coupling from another bus waveguide (comprise of add and drop ports) as labelled with E_2 in Figure 3 a). The optical electric field E_2 will coupled with the dark soliton pulse from the add port.

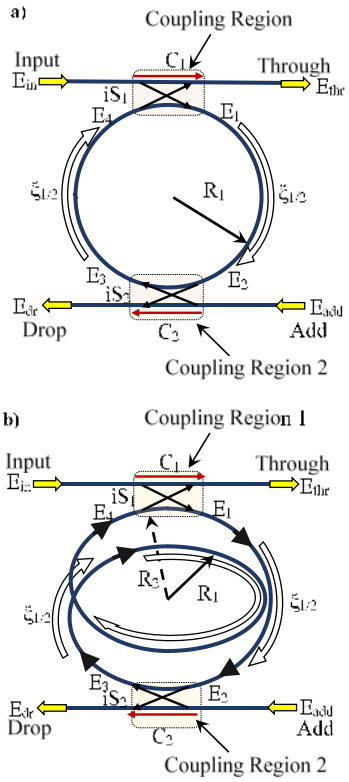

Figure 3 a) Schematics diagram of ADF microring resonator. b) Schematics diagram of ADM microring resonator

The dark soliton pulse also undergoes similar phenomenon in which it coupled into ring waveguide that illustrates by the electric field E_3 in Figure 3 a). The coupled pulse propagates in half circulation trail to the E_4 in the ADM configuration. The incident pulse of electric field E_2 is interfered with the coupled evanescence wave from the dark soliton at add port. The electric fields of the propagation pulse within the

ring waveguide can be described based on the transfer matrix method as

$$\begin{pmatrix} E_1 \\ E_{Thr} \end{pmatrix} = \begin{pmatrix} C_1 & iS_1 \\ iS_1 & C_1 \end{pmatrix} \begin{pmatrix} E_4 \\ E_{In} \end{pmatrix} \quad (7)$$

$$\begin{pmatrix} E_3 \\ E_{Dr} \end{pmatrix} = \begin{pmatrix} C_2 & iS_2 \\ iS_2 & C_2 \end{pmatrix} \begin{pmatrix} E_2 \\ E_{Add} \end{pmatrix} \quad (8)$$

For the optical fields E_1 and E3 are exhibited the half-pass phase shift $\xi_{1/2} = \exp\left[\left(-\alpha L_N / 2 - iKnL\right)/2\right]$ which travel in half circulation trails within the ring waveguide as labelled with white arrows in Fig. 3 a). The propagation distances of the ring circumferences is $L = 2\pi R_1$ per roundtrip and α attenuation constant with K as the vacuum wavenumber. The electric field E_2 *and* E_4 are expressed as

$$\begin{pmatrix} E_2 \\ E_4 \end{pmatrix} = \begin{pmatrix} \xi_{1/2} & 0 \\ 0 & \xi_{1/2} \end{pmatrix} \begin{pmatrix} E_1 \\ E_3 \end{pmatrix} \quad (9)$$

The refractive index variation is occurred as the pulse exhibited phase shift based of the nonlinear Kerr effect as shown in Equation (4). The pulse circulating power is contributed in change of the refractive index as Equation (10) [24, 25].

$$n = n_1 + n_2 \frac{\mathrm{P_r}}{A_{eff}} \quad (10)$$

The output electric fields from drop E_{dr} and output E_{Th} ports can be obtained by the expansion of transfer matrix equations as Equations (7-10).

$$E_{Th} = E_{in}\left[\frac{C_2 - C_1\xi}{1 - C_2C_1\xi}\right] - E_a\left[\frac{S_1S_2\xi_{1/2}}{1 - C_2C_1\xi}\right] \quad (11)$$

$$E_{dr} = E_a\left[\frac{C_2 - C_1\xi}{1 - C_2C_1\xi}\right] - E_{in}\left[\frac{S_1S_2\xi_{1/2}}{1 - C_2C_1\xi}\right] \quad (12)$$

In Figure 3 b), the propagation of the bright and dark soliton pulse is illustrated. Based on the transfer matrix analysis, the ADM configuration is analysed to obtain the spectrum of output signal and the optical bistability by simulating output-to-input power relation. The ADM is designed based on implementation of twisted ring waveguide that called Mobius ring into the conventional add-drop configuration. The Mobius ring waveguide consisted of circulated propagation trails with two different radius which labelled as inner R_{in} and outer R_{out} radius.as indicates in Figure 3 b).

Two circulation trails produces extra phase shift of ADM MRR configuration as compared to the ADF MRR. This is possible method to enhance the nonlinearity of MRR system which can provide the system higher build up factor. The gap ΔR between inner and outer radius should be set with higher 0.3 μm to avoid the coupling phenomenon within Mobius ring waveguide. The ADM configuration comprise near 2 times more phase shift as compared to the ADF. Based on the transfer matrix analysis, the electric fields propagation equations are given as

$$\begin{pmatrix} E_1 \\ E_{Th} \end{pmatrix} = \begin{pmatrix} C_1 & iS_1 \\ iS_1 & C_1 \end{pmatrix} \begin{pmatrix} E_4 \\ E_{In} \end{pmatrix} \quad (13)$$

$$\begin{pmatrix} E_3 \\ E_{Dr} \end{pmatrix} = \begin{pmatrix} C_2 & iS_2 \\ iS_2 & C_2 \end{pmatrix} \begin{pmatrix} E_2 \\ E_{Add} \end{pmatrix} \quad (14)$$

$$\begin{pmatrix} E_2 \\ E_4 \end{pmatrix} = \begin{pmatrix} \xi_{1/2} & 0 \\ 0 & \xi_{3/2} \end{pmatrix} \begin{pmatrix} E_1 \\ E_3 \end{pmatrix} \quad (15)$$

The extra phase shift is occurred as the electric field of the propagation pulse travels from point 3 to point 4 with half circulation trails of outer radius and full circulation trails of inner radius within the Mobius ring waveguide. Thus, by the derivation of the transfer matrix equation E_{Th} is obtained as

$$E_{Th} = E_{in}\left[\frac{C - C^2\xi^o\xi^i - CS^2\xi^o\xi^i}{1 - C^2\xi^o\xi^i}\right] - E_a\left[\frac{S^2\xi^i_{1/2}\xi^o}{1 - C^2\xi^o\xi^i}\right] \quad (16)$$

$$E_{dr} = E_a\left[\frac{C - C^2\xi^o\xi^i - CS^2\xi^o\xi^i}{1 - C^2\xi^o\xi^i}\right] - E_{in}\left[\frac{S^2\xi^i_{1/2}\xi^o}{1 - C^2\xi^o\xi^i}\right] \quad (17)$$

The output power can be defined as

$$P_{out} = \left|E_{out}\right|^2 \quad (18)$$

The switching operation will be occurred with the input threshold power which can be defined as the mean between initial to end input power of the anticlockwise hysteresis loop as Equation (12).

$$P_H = \frac{\left|P_{high} - P_{low}\right|}{2} + P_{low} \quad (19)$$

The input threshold power is decribed as the amount of input power that comprise of two stable output states which known as ON and OFF switching (P_{ON} and P_{OFF}) operation power which used to the determine the output switching power as Equation (20).

$$P_s = P_{ON} - P_{OFF} \quad (20)$$

In this present work, the comparison of output to input power relation between ADF and ADM MRR configuration are performed to observe the performance of the optical bistability effect and hysteresis loop based on the threshold and output switching power.

4.0 OPTICAL BISTABILITY

The output to input power relation of ADM and ADF MRR system is analyzed to observe the optical bistability. The system is operated with two different type of single rings, which represent ADF and ADM microring resonators. The optical bistability obtained by the soliton propagation pulses within both configurations with 200000 roundtrips and can be analysed by using the relation between optical transmission power and the controlled input sources. The optical field is fed into the ring resonator system with $50\mu m$ radius for ADF configuration and with inner radius $50\mu m$, and outer radius $51\mu m$ for ADM configuration. The coupling coefficient ratios $\kappa_1 : \kappa_2$ are $50:50$, $A_{eff} = 0.10\mu m^2$, $n_{eff} = 3.48$, $n_2 = 14.5\times10^{-18} m^2/W$ [26] (for Si/SiO_2)[27], $\alpha = 0.02\ dB$ [28], $\gamma = 0.01$, $\lambda_0 = 1.55\ \mu m$.

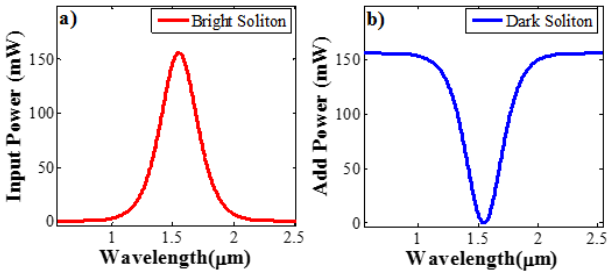

Figure 4 Optical input soliton pulses for input port and add

The optical bistability hysteresis loops are generated by the bright and dark soliton fed into the input port and add port of a microring resonator respectively as Figure 4 with the center wavelength 1.55 μm. The relation between the output signal to input is used for analyzed the optical bistability. The optical bistability effect can be found in the MRR system when the output signals of the through and drop port is controlled by optical pulses in add and input port respectively as shown in Figure 5.

At through port, optical bistability is occurred at output power P_{Thr} is 50.69 mW and add power P_{Add} is 127.80 mW for ADF configuration. In ADM MRR configuration, the bistable signal is operated at lower add power P_{Add}=104.20 mW and through power P_{Thr}=43.68 mW which shown as the white dotted and dash-line in Figure 5 a). At drop port, the ADF configuration able to obtain the optical bistability behavior of output-to-input power relation at the 53.98 mW Pth and 74.04 mW Pin which is differ with the ADM configuration. The ADM MRR configuration required 82.04 mW Pin and 86.33 mW Pth as Figure 5 b).

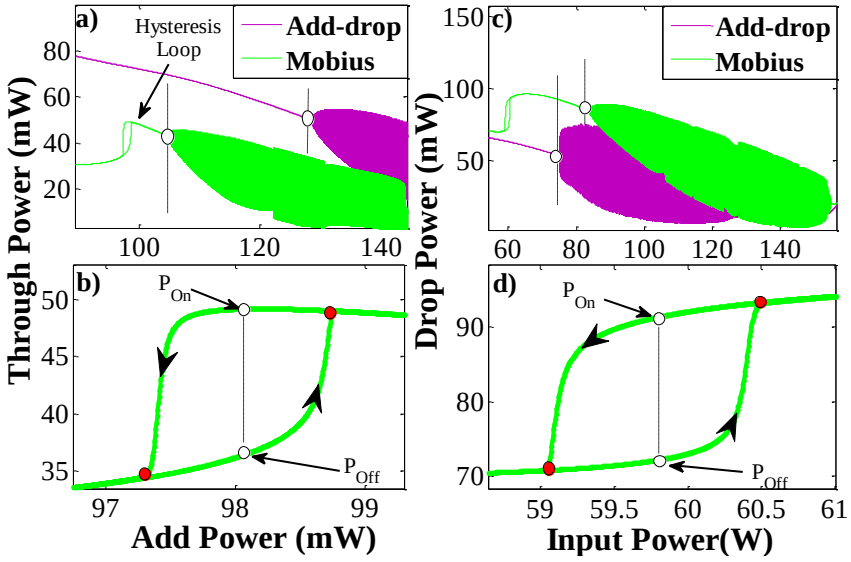

Figure 5 The optical bistable hysteresis curve with the stable state P_{on} and P_{off} at through (a) and b)) and drop port (c) and d))

The optical hysteresis loop can be generated only by using the ADM configuration which occurs in range of 97.12 mW to 98.77 mW add power P_{Add} and 34.12 mW to 49.00 mW through power P_{Th} as depicts in Figure 5 c). For drop port, the hysteresis width of bistability effect is obtained from 59.03 mW to 60.56

mW P_{In} and from 70.81 mW and 93.44 mW P_{Dr}. The mean value of the hysteresis width is used as the threshold power for the switching operation of bistable output-to-input power relation which shown as dashed line in Figures 5 b) and d). In switching operation, the input threshold power is a point that used to change the output state of optical hysteresis loop of bistable signal [29]. Two possible output power known is obtained in bistable signal as ON power P_{ON} and OFF power P_{OFF} which represented the higher and lower output power respectively as white dot in Figures 5 b) and d)

At through port, two output powers can be generated with 98.10 mW threshold power P_T are 43.45 mW and 37.98 mW as Figure 5 b). In contrast, drop port produced 56.79 mW optical threshold power P_T which is smaller than through port and generated higher ON and OFF powers which are 91.33 mW and 72.08 mW respectively. Thus, the switching power can be obtained by the computation of the difference between ON and OFF power as Equation (13). Drop port produced 19.25 mW switching power and through port generated lower switching power as 5.55 mW. The optical hysteresis loop of the ADM signals indicates the drop port and through port are possible to be used as flip-flop devices that can triggered on set and reset operation by varying the input soliton powers of the input port and add port respectively.

The increase of input power allows the optical output power triggered the set operation as the optical power increased exponentially. As the input power increase up to the end the hysteresis shape the signal has another possible output which known as reset operation of the optical flip-flop. The set switching operation can be performed by increasing the input power beyond the threshold power as shown with arrow head in Figure 5 b) and d). The increasing of the optical power will led to the electron recombination within the core material and enhance the refractive index of the material. The rise of the refractive index are increased the wavenumber and phase of the input signal and moved the Bragg resonance and photonics band to a broaden wavelength. Since the Bragg resonance wavelength becomes nearer to the input wavelength, the internal optical power is increased and induced the positive feedback of the hysteresis loop which triggered the upward switching of bistability. Thus, the positive feedback shows the increase of the nonlinear refractive index, internal optical power and the Bragg resonance which amplified the resonance signal of the system. The output signal is remained at high value P_{On} even the input signal is decreased to the initial state as threshold point P_H which illustrate in Figures 5 b) and d). The larger output signal can be obtained by new position of Bragg-resonance which increase the resonance signal. The constant decrement of carrier-density is needed to hold the position of Bragg resonance and sustain high value optical output power.

The reset operation occurs when the input power has been decreased lower than threshold power and enhances the carrier density to recover which reduce the waveguide refractive index. The Bragg resonance wavelength is reduced approaching the value of holding beam wavelength by the SPM within the system. As the resonance peak higher the signal wavelength, the positive feedback loop produces shorter Bragg resonance wavelength and lowered the output power to P_{Off} as shown in Figures 5 b) and d). The decreased input power is known as negative optical input pulse.

5.0 CONCLUSION

This work provides the analytical treatment for microring resonator system using transfer matrix method. The ADM configuration provides the greater phase change as compare to the normal ADF. It is due to the shape which comprises of 180^0 twisted. This will allows the light to exhibit the 360^0 phase change while travel in longer distance and greater bending medium. Thus, the resonant condition can be enhanced [30].Two configurations of ADM and ADF of the ring resonators are compared based on the optical bistability effect with the analyzing the output signal with respect to input signal. The ADM configuration able to surpass the performance of ADF configuration since it able to provide the optical hysteresis loop in the bistable effect. In ADM configuration, drop port produced 19.25 mW switching power and through port generated lower switching power as 5.55 mW.

Acknowledgement

We would like to thank the Laser Centre, Ibnu Sina ISIR, Universiti Teknologi Malaysia (UTM), and King Mongkut's Institute of Technology (KMITL), Thailand for providing research facilities. This research work has been supported by MyBrain15 scholarship.

References

[1] Y. A. Sharaby, A. Joshi, and S. S. Hassan. 2010. *Physics Letters A*. 37421: 2188-2194.
[2] E. Abraham and S. Smith. 1982. *Reports on Progress in Physics*. 458: 815.
[3] Y. Tanaka, H. Kawashima, N. Ikeda, Y. Sugimoto, H. Kuwatsuka, T. Hasama, and H. Ishikawa. 2006. *Ieee Photonics Technology Letters*. 1817-20: 1996-1998.
[4] M. Pollinger and A. Rauschenbeutel. 2010. *Optics Express*. 1817: 17764-17775.
[5] J. Sakaguchi, T. Katayama, and H. Kawaguchi. 2010. *Ieee Journal of Quantum Electronics*. 4611: 1526-1534.
[6] A.R. Cowan and J.F. Young. 2005. *Semiconductor Science and Technology*. 209: R41-R56.
[7] I. D. Rukhlenko, M. Premaratne, and G. P. Agrawal. 2010. *Optics Letters*. 351: 55-57.
[8] A. L. Steele. 2004. *Optics Communications*. 2361-3: 209-218.
[9] P. P. Yupapin, P. Saeung, and W. Suwancharoen. 2007. *Journal of Nonlinear Optical Physics & Materials*. 161: 111-118.

[10] Tsilipakos, O. and E.E. Kriezis. 2014. Optical Bistability With Hybrid Silicon-Plasmonic Disk Resonators. *Journal of the Optical Society of America B-Optical Physics.* 31(7): 1698-1705.
[11] M. Bahadoran, J. Ali, and P.P. Yupapin, 2013. *Applied Optics*. 5212: 2866-2873.
[12] M. Bahadoran, J. Ali, and P. P. Yupapin. 2013. *Ieee Photonics Technology Letters*. 2515: 1470-1473.
[13] J. M. Pond, S. J. Liu, and N. Newman. 2001. *Ieee Transactions on Microwave Theory and Techniques*. 4912: 2363-2368.
[14] S. Li, L. Ma, V. Fomin, S. Böttner, M. Jorgensen, and O. Schmidt. 2013. *arXiv preprint arXiv:1311.7158*.
[15] Chamorro-Posada, P., R. Gomez-Alcala, and F. J. Fraile-Pelaez. 2014. Study of Optimal All-Pass Microring Resonator Delay Lines With a Genetic Algorithm. *Journal of Lightwave Technology.* 32(8): 1477-1481.
[16] P.P. Yupapin and W. Suwancharoen. 2007. *Optics Communications*. 2802: 343-350.
[17] Aziz M. S, Jukgoljan B, Daud S, Tan TS, Ali J, Yupapin PP. 2013. Molecular Filter On-chip Design for Drug Targeting Use. *Artif Cells Nanomed Biotechnol*. 41(3):178-83.
[18] H. S. Lee, C. H. Choi, B. H. O, D. G. Park, B. G. Kang, S. H. Kim, S. G. Lee, and E. H. Lee. 2004. *Ieee Photonics Technology Letters*. 164: 1086-1088.
[19] G. P. Agrawal. 2000. *Nonlinear Fiber Optics*. Springer.
[20] M. Bahadoran, A. F. A. Noorden, K. Chaudhary, F. S. Mohajer, M. S. Aziz, S. Hashim, J. Ali, and P. Yupapin. 2014. *Sensors*. 147: 12885-12899.
[21] Y. S. Kivshar and G. Agrawal. 2003. *Optical Solitons: from Fibers to Photonic Crystals*. Academic Press.
[22] R. W. Boyd. 2003. *Nonlinear Optics*. 3rd ed. Academic Press.
[23] M. S. Aziz, S. Daud, M. Bahadoran, J. Ali, and P. P. Yupapin. 2012. *Journal of Nonlinear Optical Physics & Materials*. 214.
[24] S. Lynch. 2004. *Dynamical Systems with Applications using MATLAB®*. Birkhäuser Boston.
[25] A. Afroozeh, M. S. Aziz, M. A. Jalil, J. Ali, and P. P. Yupapin. 2011. *2nd International Science, Social Science, Engineering and Energy Conference 2010 (I-Seec 2010)*. 8: 412-416.
[26] C. Koos, L. Jacome, C. Poulton, J. Leuthold, and W. Freude. 2007. *Optics Express*. 1510: 5976-5990.
[27] H. Yates, D. Whitehead, M. Nolan, M. Pemble, E. Palacios-Lidón, S. Rubio, F. Meseguer, and C. López. *Growth and Formation of Inverse GaP and InP opals*. in *Electrochemical Society Proceedings*. 2003. Electrochemical Society.
[28] R. Palmer, L. Alloatti, D. Korn, W. Heni, P.C. Schindler, J. Bolten, M. Karl, M. Waldow, T. Wahlbrink, W. Freude, C. Koos, and J. Leuthold. 2013. *Ieee Photonics Journal*. 51.
[29] D. N. Maywar, G. P. Agrawal, and Y. Nakano. 2001. *Journal of the Optical Society of America B-Optical Physics*. 187: 1003-1013.
[30] S. J. Cooke and J. M. Pond. 2001. *Microwave and Optical Technology Letters*. 311: 6-9.